Monte Carlo study of the triangular lattice gas with first- and second-neighbor exclusions

Wei Zhang[1] and Youjin Deng[2,*]
[1]*Department of Physics, Jinan University, Guangzhou 510630, China*
[2]*Physikalisches Institut, Universität Heidelberg, Philosophenweg 12, D-69120 Heidelberg, Germany*
(Received 23 March 2008; revised manuscript received 15 June 2008; published 2 September 2008)

We formulate a Swendsen-Wang-like version of the geometric cluster algorithm. As an application, we study the hard-core lattice gas on the triangular lattice with the first- and second-neighbor exclusions. The data were first analyzed by finite-size scaling without including logarithmic corrections. We determine the critical chemical potential as $\mu_c=1.756\,82(2)$ and the critical particle density as $\rho_c=0.180(4)$. From the Binder ratio Q and susceptibility χ, the thermal and magnetic exponents are estimated as $y_t=1.51(1)\approx 3/2$ and $y_h=1.8748(8)\approx 15/8$, respectively, while the analyses of energylike quantities yield y_t ranging from 1.440(5) to 1.470(5). Nevertheless, the data for energylike quantities are also well described by theoretically predicted scaling formulas with logarithmic corrections and with exponent $y_t=3/2$. These results are very similar to the earlier study for the four-state Potts model on the square lattice [J. Stat. Phys. **88**, 567 (1997)], and strongly support the general belief that the model is in the four-state Potts universality class. The dynamic scaling behavior of the Metropolis simulation and the combined method of the Metropolis and the geometric cluster algorithm is also studied; the former has a dynamic exponent $z_{\mathrm{int}}\approx 2.21$ and the latter has $z_{\mathrm{int}}\approx 1.60$.

DOI: 10.1103/PhysRevE.78.031103 PACS number(s): 05.50.+q, 05.10.Ln, 02.70.Rr, 05.20.Gg

I. INTRODUCTION

Lattice gases, together with the Potts (including Ising) and the $O(n)$ model, play an important role in the statistical mechanics. They are used to describe universal properties of many complex physical systems, ranging from simple fluids to structural glasses and granular materials. Lattice-gas models are generally defined as follows. For a given lattice, a number of particles is randomly distributed over its vertices with the constraint that each vertex can at most be occupied by one particle; the density of particles is controlled by the chemical potential μ. Particles on different vertices can interact with one another—normally through two-body interactions. Accordingly, the reduced Hamiltonian (already divided by kT with Boltzmann factor k and temperature T) of a lattice-gas model can be written as

$$\mathcal{H}=-\mu\sum_i \sigma_i - K_{1N}\sum_{\{jk\}}\sigma_j\sigma_k - K_{2N}\sum_{\{lm\}}\sigma_l\sigma_m+\cdots, \quad (1)$$

where $\sigma=0,1$ represents the absence and the presence of a particle, respectively. The second term with amplitude K_{1N} describes the first-neighbor interactions, and the third one with K_{2N} is for the second-neighbor couplings; further-neighbor interactions can be included, as denoted by the symbol "$\cdots$."

In the study of lattice gases, one often takes the hard-core limit: in Eq. (1) the couplings K outside a certain range ($r>r_0$) are set zero, while $K(r\leqslant r_0)$ is taken to the limit $K\to-\infty$; namely, the particles have a hard-core of radius r_0. A particular example is the lattice-gas model with nearest-neighbor exclusion: $K_{1N}\to-\infty$ while all further-neighbor couplings are zero. Unlike the Potts model and the $O(n)$ spin model, the nature and the universality of the phase transitions of lattice-gas systems depend on the underling lattice structures. For instance, the lattice-gas model with nearest-neighbor exclusions on the square and on the honeycomb lattice is believed to be Ising-like, while that on the triangular lattice (Baxter's hard-hexagon model [1,2]) belongs to the three-state Potts universality class.

Extensive investigations have been carried out for lattice gases, and many theoretical and numerical approaches are applied. This includes exact calculations (mainly by Baxter and coauthors), series expansions (like high-temperature and low-temperature expansions), cluster variation method, transfer matrix calculations, and Monte Carlo simulations, etc. The critical free energy of Baxter's hard-hexagon lattice gas was exactly calculated [1,3–5]; the critical chemical potential is known as $\mu_c=\ln[(11+\sqrt{5})/2]$, and the critical particle density is $\rho_c=(5+\sqrt{5})/10$. Baxter's hard-square model [1,3–5], defined by Eq. (1) on the square lattice with $K_{1N}\to-\infty$ and finite K_{2N}, is known to have a tricritical point $(\mu_{tc},K_{2N,tc})$ in the tricritical Ising universality class; the tricritical point lies at $\mu_{tc}=-\ln[8(1+\sqrt{5})]$, $K_{2N,tc}=\ln(3+\sqrt{5})$, with $\rho_{tc}=(5+\sqrt{5})/10$. Using the transfer-matrix technique, Guo and co-authors [6] determine the critical point of the hard-core square lattice gas up to the 11th decimal place, $\mu_c=1.334\,015\,100\,277\,74(1)$, $\rho_c=0.367\;742\,999\,041\,0(3)$. Recently, Monte Carlo simulations were carried out for square lattice gases with the hard-core radius up to the fifth neighbors [7]. The nature of phase transitions was found to be continuous for exclusions up to $1N$, to $2N$, and to $4N$, and to be discontinuous for exclusions up to $3N$ and $5N$, where symbols iN represents the ith neighbors.

In this work, we shall consider the hard-core lattice gas on the triangular lattice with the first- and second-neighbor repulsions. The triangular lattice in this case can be divided into four sublattices (see Fig. 1), and for sufficiently high density particles prefer to occupying one of the four sublattices. Thus one would expect that, if it is second order, the melting of ordered phase should be in the four-state Potts universality class. However, several studies at the end of the 1960s last century suggested that the phase transition is first order [8,9]. Later, Bartelt and Einstein [10] reexamined this model by a phenomenological renormalization–transfer-

*yd10@nyu.edu

 ©2008 The American Physical Society

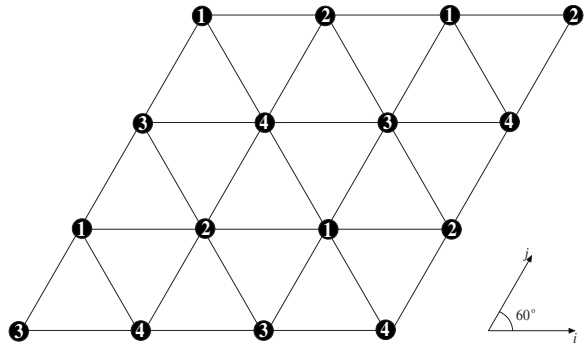

FIG. 1. The triangular lattice and its four sublattices. For chemical potential $\mu \to \infty$, one of the sublattices is fully occupied.

matrix scaling. The largest system size in their study is $16 \times \infty$. Slowly convergent finite-size corrections were observed. It was estimated that the thermal and the magnetic critical exponents are $y_t = 1.400$ and $y_h = 1.885$, respectively. Despite the noticeable deviations from the exact values $y_t = 3/2$ and $y_h = 15/8$ [11,12], these estimates are in favor of the four-state Potts universality in view of the possible occurrence of logarithmic corrections.

Here, we aim to provide an independent study of this model by means of Monte Carlo simulations. This seems justified since no rigorous argument exists about the nature of the phase transition and the evidence in Ref. [10] is not very strong. To properly analyze finite-size corrections, more accurate numerical data, particularly for large system sizes, are desirable. [Sometimes, when finite-site corrections are not properly taken into account, wrong conclusions can be reached. For instance, from the Metropolis simulations of the lattice-gas model on the simple-cubic lattice with the first-neighbor repulsions, Yamagata estimated the critical exponents as $\beta/\gamma = 0.311(8)$ and $\gamma/\nu = 2.38(2)$ [13], which would imply $y_h = 2.689(8)$. This result is significantly different from the general accepted value $y_h = 2.4816(2)$ for the Ising universality class in three dimensions [14].] Our task becomes now feasible because of the availability of the efficient cluster algorithm for lattice-gas models—the geometric cluster algorithm—and the rapid development of the computer industry in the past few decades. The geometric cluster algorithm [15,16] moves around a fraction of particles over the lattice according to geometric symmetries, such as the spatial inversion or rotation symmetries of the triangular lattice; a detailed description will be given in Sec. II. The algorithm does not change the total number of particles, and it is combined with the Metropolis steps in order to simulate lattice-gas systems in the grand-canonical ensemble. In comparison with simulations using the Metropolis method only, critical slowing down is significantly suppressed. Therefore we are able to simulate systems as large as 480×480 within reasonable computer resources.

II. GEOMETRIC CLUSTER ALGORITHM AND SAMPLED QUANTITIES

A. Geometric cluster algorithm

The geometric cluster algorithm was first proposed by Dress and Krauth [17] in the study of hard-core gases in continuous space. Unlike the well-known Swendsen-Wang (SW) cluster method which flips spins, the elementary operation in this algorithm is to move particles. For hard disks, the percolation threshold of the cluster formation process deviates significantly from the phase transition of the model. This is unfortunate since it affects the efficiency of the algorithm.

A single-cluster version of the geometric cluster algorithm was later developed by Heringa and Blöte [15,16] for lattice models like the Potts model and the lattice gases. Here, we shall briefly describe it in terms of the lattice-gas model (1) with a soft-core radius of a lattice unit (finite $K: \equiv K_{1N} < 0$ and all other couplings are zero) on the square lattice with periodic boundary conditions. For such a geometry, one can set a Cartesian coordinate by taking any two perpendicular lines of lattice sites as the x and the y axis, respectively. It can be seen that the Hamiltonian of the system is invariant under geometric operations like reflections about the x or the y axis or inversion about the center of the coordinate. Further, any configuration will be restored if an operation is subsequently applied twice—namely, these operations are self-inverse. One can employ any of such geometric operations to formulate a cluster algorithm. Let a pair of nearest-neighboring sites i,k be mapped onto i',k', respectively. One denotes the energy difference when a neighbor k of i is interchanged with k' as Δ_{ik}, which is $\Delta_{ik} = K(\sigma_i\sigma_k + \sigma_{i'}\sigma_{k'} - \sigma_i\sigma_{k'} - \sigma_{i'}\sigma_k)$. The algorithm then involves the following steps:

1. Choose a random site i: both i and i' belong to the cluster.

2. Interchange σ_i and $\sigma_{i'}$.

3. For all neighbors k of i that do not belong to the cluster yet, do the following:

(i) If $\Delta_{ik} > 0$, do the following with probability $p = 1 - \exp(-\Delta_{ik})$: (a) interchange σ_k and $\sigma_{k'}$ (k and k' are included in the cluster), (b) write k in a list of addresses (called the stack).

(ii) If $\Delta_{ik} < 0$, do nothing.

4. Read an address j from the stack. Substitute j for i, and execute step 3.

5. Erase j from the stack.

6. Repeat Steps 4 and 5 until the stack is empty.

When the stack is empty, the cluster is completed. Since the elementary operation is to interchange spins σ_i and $\sigma_{i'}$, the total number of particles does not change in the algorithm. For the above geometric cluster steps, the detailed balance has already been proved [15,16]. The efficiency of this algorithm for different models has also been demonstrated. For the Ising model, it was shown that the percolation of the formed clusters coincides with the thermal phase transition, reflecting the efficiency of the algorithm. In fact, in the canonical ensemble (the total number of particles is fixed), it can be shown that, for many models, no critical slowing down exists for some quantities [18].

Here we shall formulate a full-cluster version of the geometric cluster algorithm in an analogous way as the Edward-Sokal picture for the well-known SW cluster method for the ferromagnetic Potts model [19,20]. We consider the lattice-gas model (1) with finite nearest-neighbor interactions ($K: \equiv K_{1N} < 0$) on a one-dimensional chain with sites labeled as $i = \pm 1/2, \pm 3/2, \pm 5/2, \ldots$. Instead of writing the Hamil-

TABLE I. Energies $\mathcal{E}_1$ and $\mathcal{E}_2$ of a building block in Eq. (2). The associated bond weight for $K<0$ in the geometric cluster algorithm is also given. In the "Example," the upper two sites are i and $i+1$, and the lower are $-i$ and $-i-1$. The filled (empty) circle represents the presence (absence) of a particle.

Case	1	2	3	4	5	6	7
	0 particle	1 particle		2 particles		3 particles	4 particles
Example	○-○ ○-○	●-○ ○-○	●-○ ●-○	●-● ○-○	●-○ ○-●	●-● ●-○	●-● ●-●
$\mathcal{E}_1$	0	0	0	$-K$	0	$-K$	$-2K$
$\mathcal{E}_2$	0	0	0	0	$-K$	$-K$	$-2K$
v	0	0	0	0	$e^{-K}-1$	0	0

tonian for a fixed number of particles as a sum of the nearest-neighbor couplings like in Eq. (1), we rewrite it as

$$\mathcal{H}|_{N_p=N} = \sum_{i=1/2}^{\infty} \mathcal{H}_i = -K \sum_{i=1/2}^{\infty} (\sigma_i \sigma_{i+1} + \sigma_{-i}\sigma_{-i-1}), \quad (2)$$

where $N_p=\Sigma_i \sigma_i$ and the constant N denotes the total number of particles. The Hamiltonian (2) is obtained by applying the reflection about the center $i=0$—*a* geometric operation. In this form, the "building blocks" of the Hamiltonian is no longer a pair of neighboring sites, but two pairs of them. If one only uses the spin-interchange operation $\eta: \equiv \sigma_i \leftrightarrow \sigma_{-i}$, the energy associated with each building block is of two levels at most: $\mathcal{E}_1(\vec{\sigma}): \equiv -K(\sigma_i\sigma_{i+1}+\sigma_{-i}\sigma_{-i-1})$ and $\mathcal{E}_2(\vec{\sigma}): \equiv -K(\sigma_i\sigma_{-i-1}+\sigma_{-i}\sigma_{i+1})$. The former $\mathcal{E}_1$ refers to the status that no operator η is applied or it is applied at both vertices i and j; instead, the latter $\mathcal{E}_2$ means that η is applied at i (or j) only. The values of $\mathcal{E}_1$ and $\mathcal{E}_2$ depend on the spin configuration $\vec{\sigma}$ on the building block. For the lattice-gas mode (2), these values are shown in Table I. Let us denote the lower and the upper level of $\mathcal{E}_1$ and $\mathcal{E}_2$ as $\mathcal{E}_{\text{low}}$ and $\mathcal{E}_{\text{upp}}$, respectively. The statistical weight associated with each block in Eq. (2) reads

$$e^{-\mathcal{H}_i(\vec{\sigma})} = e^{-\mathcal{E}_{\text{upp}}}(1 + v_i \delta_{\mathcal{E}_1,\mathcal{E}_{\text{low}}}) \quad \text{with } (v_i = e^{\mathcal{E}_{\text{upp}}-\mathcal{E}_{\text{low}}} - 1). \quad (3)$$

On this basis, the partition sum becomes

$$\mathcal{Z}|_{N_p=N} = \sum_{\{\sigma\}:N_p=N} \prod_{i=1/2}^{\infty} e^{-\mathcal{E}_{\text{upp}}(\vec{\sigma})} \prod_{i=1/2}^{\infty} (1 + v_i \delta_{\mathcal{E}_1,\mathcal{E}_{\text{low}}}). \quad (4)$$

Analogously as mapping the Potts model onto the random-cluster model, one introduces a bond variable b_i to graphically represent the expansion of the second product in Eq. (4): if the term $v_i\delta_{\mathcal{E}_1,\mathcal{E}_{\text{low}}}$ is taken, an occupied bond $b_i=1$ is placed between sites i and $i+1$; otherwise, no bond is placed ($b_i=0$). This leads to a joint model

$$\mathcal{Z}|_{N_p=N} = \sum_{\{\sigma\}:N_p=N} \prod_{i=1/2}^{\infty} e^{-\mathcal{E}_{\text{upp}}(\vec{\sigma})} \sum_{\{b\}} (v_i \delta_{\mathcal{E}_1,\mathcal{E}_{\text{low}}})^{b_i}, \quad (5)$$

where the second sum is over all possible bond configurations that are consistent with the spin configuration, and we have already assumed the conventional symbol $0^0=1$. Given a spin configuration $\{\sigma\}$, the expression (5) allows us to place bonds and construct clusters as follows: if the spin configuration on a block i is at the lower-energy level $\mathcal{E}_{\text{low}}$, one places a bond $b_i=1$ with probability $v_i/(1+v_i)$; otherwise, place no bonds. Note that a bond connects four lattice sites, since it is placed on the blocks. Lattice sites connected through a chain of occupied bonds form a cluster. The condition $\delta_{\mathcal{E}_1,\mathcal{E}_{\text{low}}}=1$ for a block can be held either by doing nothing or interchanging both spins ($\sigma_i \leftrightarrow \sigma_{-i}$, $\sigma_{i+1} \leftrightarrow \sigma_{-i-1}$). Thus for a spin-jointed-bond configuration, for each cluster one has the freedom to choose the do-nothing or the spin-interchange operation, and apply it to *all* lattice sites within the cluster. Accordingly, a Swendsen-Wang-like geometric cluster algorithm can be formulated as follows.

1. Choose a geometric transformation such that every building block in the Hamiltonian consists of two pairs of neighboring couplings and the associated energy is only of two levels under the spin-interchange operation.

2. For each building block i (containing four lattice sites), if its spin configuration is at the lower-energy $\mathcal{E}_{\text{low}}$, place a bond with probability $p_i=v_i/(1+v_i)$; otherwise, place no bond.

3. Construct clusters according to the occupied bonds.

4. Independently for each cluster, randomly choose the do-nothing or the spin-interchange operation with probability 1/2; apply the chosen operation to all lattice sites within the cluster.

A Monte Carlo step is completed, and a new spin configuration is obtained.

We hope that the analogy between our formulation of the geometric cluster algorithm and the well-known SW method can help the reader to understand better the geometric cluster algorithm. Further, except for the Ising case, it is not *a priori* clear whether the percolation threshold of the geometric clusters coincides with the associated thermal transition. (For many systems, we have some preliminary numerical results that the thermal transition and the percolation threshold of geometric clusters do not coincide. A detailed study seems desirable cut out of the scope of the present work.) Accordingly, it is not clear which version (SW or single-cluster) of the geometric cluster algorithms is more efficient.

We conclude this subsection by mentioning the following. (i) Like the SW method for the ferromagnetic Potts model, the essence in the geometric cluster process is that the energy

of each building block has two levels only under the spin-interchange operation (the energy of a building block may have more than two levels if other operations—like the spin-flip operation—are allowed). (ii) Normally, the rewriting of the Hamiltonian as a sum of proper building blocks is obtained by applying some global geometric transformation, such as the inversion about the center and reflection, etc. (iii) In the canonical ensemble, if one uses the geometric cluster algorithm only, a large number of spatial transformations should be available such that each lattice site in a system should be able to reach any other lattice site by a finite number of geometric mappings. For the torus geometry, this can be easily achieved since any site can serve as the center of the aforementioned Cartesian coordinate. In the case that the geometric cluster method is itself nonergodic, it can be combined with other algorithms like the Kawasaki dynamic. (iv) For simulations in the grand-canonical ensemble, other Monte Carlo methods have to be used.

B. Sampled quantities

For the lattice-gas model (1), the triangular lattice is divided into four sublattices. The particle density is then sampled as

$$\rho^{(i)} = \frac{4}{V} \sum_{k \in \mathcal{T}^{(i)}} \sigma_k, \tag{6}$$

where $V=L\times L$ is the volume of the lattice and the sum is over each sublattice, labeled as $i=1,2,3,4$. The global particle density is then $\rho=(\rho^{(1)}+\rho^{(2)}+\rho^{(3)}+\rho^{(4)})/4$. On this basis, we measured the second and the fourth moment of the magnetization density as

$$\mathcal{M}^2 = \frac{1}{3}\sum_{i=1}^{3}\sum_{j=i+1}^{4}(\rho^{(i)}-\rho^{(j)})^2 \quad \text{and } \mathcal{M}^4 = (\mathcal{M}^2)^2, \tag{7}$$

where factor $1/3$ is for normalization purpose such that $\mathcal{M}^2$ is a unity when the chemical potential is infinite-one of the four sublattices is fully occupied. The magnetic susceptibility is $\chi=V\langle\mathcal{M}^2\rangle$. Then, we define a dimensionless ratio as

$$Q = \frac{\langle\mathcal{M}^2\rangle^2}{\langle\mathcal{M}^4\rangle}. \tag{8}$$

This ratio at criticality approaches a universal value for $L\to\infty$, and is known to be very useful in estimating critical points.

Since a pair of first- (or second-) neighboring sites cannot both be occupied by particles, we sampled the third-neighbor correlation as an energylike quantity

$$\mathcal{E} = \frac{1}{6V}\sum_{\{ij\}\in 3N}\sigma_i\sigma_k, \tag{9}$$

where the sum is over all the third-neighbor pairs. Correspondingly, a specific-heat-like quantity is defined as $\mathcal{C}_e = V(\langle\mathcal{E}^2\rangle-\langle\mathcal{E}\rangle^2)$. We also measured the compressibility $\mathcal{C}_v = V(\langle\rho^2\rangle-\langle\rho\rangle^2)$.

Finally, let us define the quantities associated with the Monte Carlo dynamics. Given an observable $\mathcal{O}$, we define the corresponding unnormalized autocorrelation function as

$$\mathcal{C}_{\mathcal{O}\mathcal{O}}(t) = \langle\mathcal{O}_s\mathcal{O}_{s+t}\rangle - \langle\mathcal{O}\rangle^2, \tag{10}$$

where t is the time in units of Monte Carlo steps. The associated normalized autocorrelation function is

$$\rho_{\mathcal{O}\mathcal{O}}(t) = \frac{\mathcal{C}_{\mathcal{O}\mathcal{O}}(t)}{\mathcal{C}_{\mathcal{O}\mathcal{O}}(0)}. \tag{11}$$

The integrated autocorrelation time for the observable $\mathcal{O}$ is defined as

$$\tau_{\text{int},\mathcal{O}} = \frac{1}{2}\sum_{t=-\infty}^{\infty}\rho_{\mathcal{O}\mathcal{O}}(t). \tag{12}$$

The integrated autocorrelation time controls the statistical error in Monte Carlo estimates of the mean $\langle\mathcal{O}\rangle$.

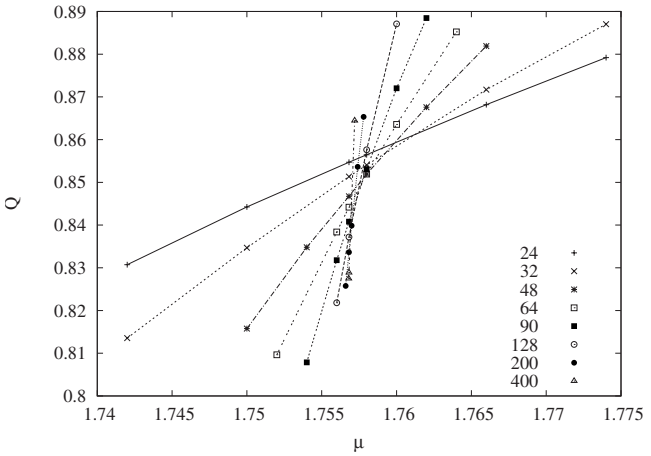

FIG. 2. Ratio Q vs μ for various system sizes. The straight line segments, simply connecting the data points, are for illustration purpose.

III. RESULTS

Using a combination of the Metropolis and the geometric cluster algorithm, we simulated the lattice-gas model on the triangular lattice with first- and second-neighbor repulsions. Periodic boundary conditions were used in the rhombus geometry shown in Fig. 1. System sizes took 16 values in range $8\leqslant L\leqslant 480$. Significant critical slowing down was observed.

Some primary simulations for relatively small system sizes were first carried out to find the approximate location of the critical point from the intersection of the Q data for different system sizes L (we were also guided by the result $\mu_c\approx 1.7599$ in Ref. [10]). Then extensive simulations for large sizes were performed near $\mu_c=1.757$.

A. Analyses without logarithmic corrections

Figure 2 shows parts of the Monte Carlo data of the dimensionless ratio Q. According to the least-squares criterion, the Q data were fitted by

$$Q(\mu,L) = Q_c + q_1(\mu-\mu_c)L^{y_t} + q_2(\mu-\mu_c)L^{2y_t} + b_1L^{y_1} + b_2L^{y_2} + b_3L^{y_3} + r_1L^{y_r} + c_1(\mu-\mu_c)L^{y_t+y_1}, \quad (13)$$

where q_i, b_i, c_i, and r_i are unknown parameters, and Q_c is the universal value. The terms with q_i describe the contributions of the thermal field due to deviation from the critical point, those with exponent y_i account for finite-size corrections, and the one with c_1 is for the mixed effect of the relevant and irrelevant thermal fields. The term with exponent $y_r=d-2y_h$ arises from the regular part of the free energy, where the magnetic exponent y_h was fixed at 15/8 for the four-state Potts model. The detailed derivation of the finite-size scaling formula (13) can be found in Ref. [14]. From the numerical results for the tricritical four-state Potts model [18] where the marginal field is absent, we learn that there exist correction terms with exponent $y_1=-1$. Thus we set $y_1=-1$, $y_2=-2$, and $y_3=-3$.

Since the transition is expected to be in the four-state Potts universality class, one should in principle include logarithmic corrections in Eq. (13), which is, however, by no means an easy task. It was derived [21] that, for the four-state Potts model near criticality, not only the leading power-law scaling behavior is modified by multiplicative logarithms, but there exist additive correction terms of form lnln/ln and 1/ln. In Ref. [21], the four-state Potts model on the square lattice was studied by Monte Carlo simulations with linear size in range $4\leqslant L\leqslant 1024$. The authors [21] could not disentangle these logarithmic corrections; they found that, for such a purpose, one would need to reach at least $L\approx 10^{64}$!

Satisfactory fits of the Q data by Eq. (13) can be obtained after a cutoff for small system sizes $L<18$, which yield $\mu_c=1.756\,82(2)$, $y_t=1.51(1)\approx 3/2$, and $Q_0=0.823(2)$. It is interesting to observe that, without logarithmic corrections, satisfactory fits can include data for rather small sizes and the exponent $y_t=1.51(1)$ agrees well with the exact value 3/2. This suggests that logarithmic corrections are small in the Q data, and thus the fitting results for Q are more or less reliable.

We then fitted the χ data by

$$\chi = \chi_0 + L^{2y_h-2}[a_0 + a_1(\mu-\mu_c)L^{y_t} + a_2(\mu-\mu_c)L^{2y_t} + b_1L^{y_1} + b_2L^{y_2} + c_1(\mu-\mu_c)L^{y_t+y_1}], \quad (14)$$

where χ_0 stems from the regular part of the free energy, which acts in Eq. (13) as a correction term with exponent $y_r=2-2y_h$. The correction exponents were also set as $y_1=-1$ and $y_2=-2$. After a cutoff for small systems $L<20$, we obtain $\mu_c=1.756\,83(1)$, $y_t=1.489(9)\approx 3/2$ and $y_h=1.8748(8)\approx\frac{15}{8}$. The estimate of μ_c is consistent with that from Q, and those for y_t and y_h agree with the exact values. If the exponent y_t is fixed at 3/2, one has $\mu_c=1.756\,83(1)$ and $y_h=1.8743(7)$ after discarding the data for $L<18$.

The data for the particle density ρ were fitted by

$$\rho = \rho_0 + \rho_1(\mu-\mu_c) + L^{y_t-d}[a_0 + a_1(\mu-\mu_c)L^{y_t} + a_2(\mu-\mu_c)L^{2y_t} + b_1L^{-1} + b_2L^{-2} + b_3L^{-3}]. \quad (15)$$

Satisfactory fits are obtained after a cutoff for small systems $L<16$, and we have $\mu_c=1.756\,82(2)$, $y_t=1.440(5)$, and $\rho_c=0.180(4)$. The result $\mu_c=1.756\,80(3)$ agrees well with those obtained from magnetic quantities Q and χ. However, the value $y_t=1.440(5)$ significantly differs from 3/2.

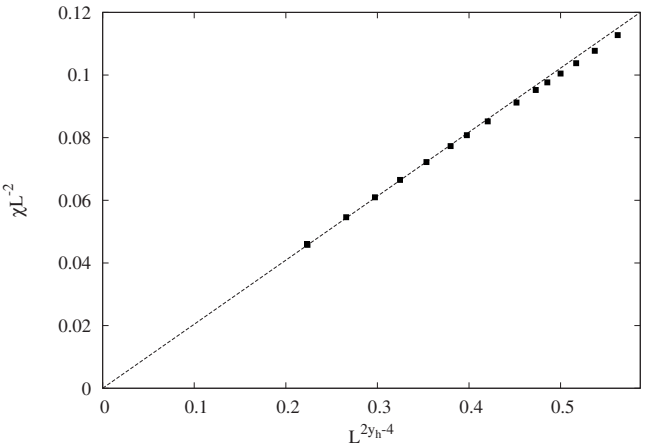

FIG. 3. Quantity χ/L^2 at $\mu=1.756\,818$ vs L^{2y_h-4}, with $y_h=15/8$. The statistical error bars are smaller than the size of the data points. The dashed line is just for illustration purpose.

The finite-size scaling formula of the specific-heat-like quantities C_e and C_v reads

$$C = r_0 + r_1(\mu-\mu_c) + L^{2y_t-d}[a_0 + a_1(\mu-\mu_c)L^{y_t} + a_2(\mu-\mu_c)L^{2y_t} + a_3(\mu-\mu_c)L^{3y_t} + b_1L^{-1} + b_2L^{-2} + b_3L^{-3} + c_1L^{y_t-1}(\mu-\mu_c)]. \quad (16)$$

In the actual fits, the terms r_0, arising from the regular part of free energy, cannot be distinguished from the correction term $b_1L^{2y_t-d-1}=b_1$, and so is for r_1 and c_1. Thus we simply set r_0 and r_1 to be zero. The data for $L\geqslant 18$ are well described by Eq. (16). The fits for C_v yield $\mu_c=1.756\,82(3)$, $y_t=1.468(7)$ and those for C_e yield $\mu_c=1.756\,80(2)$, $y_t=1.470(5)$. Again, the estimates of μ_c agree well with those from other quantities, while the values of y_t differ significantly from 3/2.

We have simulations at $\mu=1.756\,818$, at criticality within the estimated error bars. Thus we could analyze various quantities right at the critical point. The finite-size scaling behavior of χ, ρ, and C_e and C_v at criticality is given by Eqs. (14)–(16), respectively, by throwing out those μ-dependent terms. The estimates of the associated critical exponents from these simplified analyses are consistent with those from the aforementioned fits. Figures 3 and 4 show the critical χ and C_e data, respectively. The fitting results are summarized in Table II.

We mention that the Monte Carlo data for the critical four-state Potts model on the square lattice were also analyzed [21] by finite-size scaling without logarithmic corrections. The results are $y_h=1.8720(5)$ from susceptibility and $y_t=1.385(5)$ from the specific heat. By comparing these results with our estimates of y_h and y_t, we are more convinced that the triangular-lattice gas with the first- and second-neighbor exclusions is in the four-state Potts universality class, and that the deviations of y_t from the exact value 3/2 are due to logarithmic corrections.

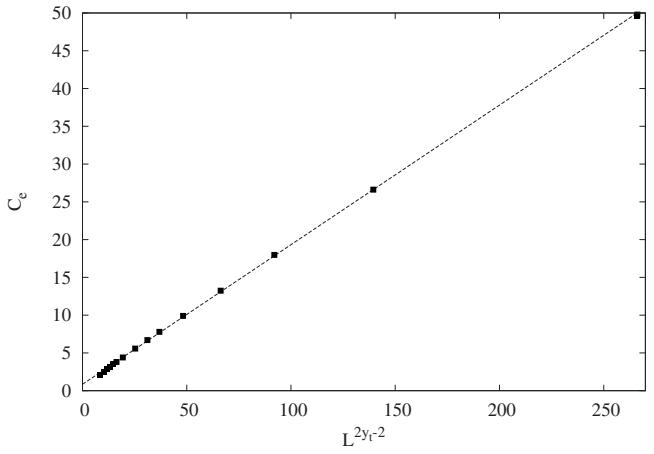

FIG. 4. Specific-heat-like quantity C_e at $\mu=1.756\,818$ vs L^{2y_t-2}, where the value of $y_t=1.470$ is taken from the fit. The statistical error bars of the data points are in the same order of their size. The dashed line is for illustration purpose.

B. Analyses with logarithmic corrections

It was derived [21] that, at criticality, the finite-size scaling of energy density $\mathcal{E}$, specific-heat-like quantities C, and susceptibility χ reads

$$\mathcal{E} = \mathcal{E}_0 + \frac{L^{y_t-2}}{(a_t+\ln L)^{3/4}}\left[b_{0e} + b_{1e}\frac{\ln\ln L}{\ln L} + b_{2e}\frac{1}{\ln L} + \cdots\right], \tag{17}$$

$$C = C_0 + \frac{L^{2y_t-2}}{(a_t+\ln L)^{3/2}}\left[b_{0c} + b_{1c}\frac{\ln\ln L}{\ln L} + b_{2c}\frac{1}{\ln L} + \cdots\right], \tag{18}$$

and

$$\chi = \chi_0 + \frac{L^{2y_h-2}}{(a_h+\ln L)^{1/8}}\left[b_{0h} + b_{1h}\frac{\ln\ln L}{\ln L} + b_{2h}\frac{1}{\ln L} + \cdots\right], \tag{19}$$

where constants "a"s and "b"s are nonuniversal and $\mathcal{E}_0$, C_0, and χ_0 are from the regular part of the free energy density.

We fitted the C_e and C_v data by Eq. (18) with b_{1c} and b_{2c} fixed at zero; by throwing data for $L\leqslant 60$, we obtain $y_t=1.565(8)$, which is now bigger than 3/2. If a_t, b_{0c}, and b_{1c} were free to be determined in the fit, the fitting procedure would fail to work properly and do not give meaningful estimates of these parameters, due to the limited data.

We found that, by respectively fixing $a_t=11$ and 7, the C_e and the C_v data are well described by Eq. (18) with $y_t=1.504(7)$ and $b_{1c}=b_{2c}=0$. Analogously, by respectively fixing $a_t=11$ and 7, we fitted Eq. (17) to the $\mathcal{E}$ and the ρ data at criticality. For $L\geqslant 24$ we obtain $y_t=1.51(2)$, in agreement with 3/2.

IV. DYNAMIC SCALING AT CRITICALITY

In this section, we shall analyze briefly the dynamic critical behavior of the Metropolis algorithm and of a combination of the Metropolis and the geometric cluster algorithm for the triangular lattice gas with the first- and second-neighbor exclusions; for the latter a Monte Carlo step consists of a Metropolis and a geometric-cluster sweep. The simulations were performed at $\mu=1.756\,818$. System sizes took six values in the range $12\leqslant L\leqslant 240$ for the Metropolis algorithm and seven values in $12\leqslant L\leqslant 480$ for the combined method. We computed the autocorrelation functions $\rho_{\mathcal{E},\mathcal{E}}(t)$ for the energy density, $\rho_{\rho,\rho}(t)$ for the particle-number density, and $\rho_{\chi,\chi}(t)$ for the susceptibility, and the associated integrated autocorrelation times $\tau_{\mathrm{int},\mathcal{E}}$, $\tau_{\mathrm{int},\rho}$, and $\tau_{\mathrm{int},\chi}$.

When simulations use the Metropolis algorithm only, one expects that both fluctuations of the total particle number (energylike mode) and the particle-number fluctuations between different sublattices (magnetic mode) attribute critical slowing down. Accordingly, the dynamic exponents z_{int}, which describes the scaling behavior of integrated autocorrelation times as $\tau_{\mathrm{int}}\propto L^{z_{\mathrm{int}}}$, has a lower bound $z_{\mathrm{int}}\geqslant 2y_h-2=7/4$. The geometric cluster algorithm moves particles among different sublattices, and thus can help to relax the magnetic mode for the critical slowing down. Therefore we expect that the lower bound of z_{int} comes from the energylike mode, i.e., $z_{\mathrm{int}}\geqslant 2y_t-2=1$ [22].

The $\tau_{\mathrm{int},\mathcal{E}}$, $\tau_{\mathrm{int},\rho}$, and $\tau_{\mathrm{int},\chi}$ data for the Metropolis algorithm are shown in Table III, and were fitted by

$$\tau_{\mathrm{int}}(L) = \tau_0 + AL^{z_{\mathrm{int}}}, \tag{20}$$

with τ_0 and A nonuniversal constants. Satisfactory fits are obtained for $L\geqslant 24$, and yield $z_{\mathrm{int},\mathcal{E}}=2.21(4)$, $z_{\mathrm{int},\rho}=2.22(4)$, and $z_{\mathrm{int},\chi}=2.09(9)$.

TABLE II. Fitting results for various quantities. Symbol $L_{\min}$ is the minimum system size for which the Monte Carlo data are included in the fit.

Quantity	$L_{\min}$	μ_c	ρ_c	y_t	y_h
Q	20	1.75682(2)		1.51(1)	
χ	20	1.75683(1)		1.489(9)	1.8748(8)
ρ	18	1.75680(3)	0.180(4)	1.440(5)	
$\mathcal{E}$	12	1.75680(2)		1.48(2)	
C_e	18	1.75680(2)		1.470(5)	
C_v	18	1.75682(3)		1.468(7)	
Previous		1.7599		1.400	1.885

TABLE III. Integrated correlation times τ_{int} for the Metropolis algorithm.

L	$\tau_{\text{int},\mathcal{E}}$	$\tau_{\text{int},\rho}$	$\tau_{\text{int},\chi}$
12	46.1(4)	41.8(4)	55.6(5)
18	121(1)	112(1)	149(2)
24	231(3)	217(2)	287(4)
30	392(5)	372(5)	492(7)
42	829(12)	795(12)	1033(17)
60	1896(33)	1835(11)	2347(46)
120	8823(250)	8667(245)	10648(301)
240	39312(1836)	38455(1818)	43525(2157)

The numerical data for the combined method of the Metropolis and the geometric-cluster algorithm are shown in Table IV and were fitted by Eq. (20). We obtain $z_{\text{int},\mathcal{E}}=1.61(3)$, $z_{\text{int},\rho}=1.61(4)$, and $z_{\text{int},\chi}=1.58(3)$.

V. DISCUSSION

In the language of the lattice gas systems, we formulate a Swendsen-Wang-like version of the geometric cluster algorithm that has already found many applications [18,23]. Since our formulation is in line with the Swendsen-Wang algorithm for the ferromagnetic Potts model, we expect that it will help the reader to understand the geometric cluster method.

We then study the triangular lattice gases with the first- and second-neighbor exclusion, using a combination of the Metropolis and the geometric cluster algorithm. The estimated critical point $\mu_c=1.756\,82(2)$ significantly improves over the existing result 1.7599; to our knowledge, no report has been published yet for the critical particle density $\rho_c=0.180(4)$. The excellent agreement between the exact values and the numerical estimates $y_t=1.51(1)$ and $y_h=1.8743(7)$ give strong support for the expectation that the model is in the four-state Potts universality class. On the other hand, the fitting results from energylike quantities imply that, although additive logarithmic corrections might be small, multiplicative logarithmic corrections cannot be neglected at least in energylike quantities.

TABLE IV. Integrated correlation times τ_{int} for the combined method of the Metropolis and the geometric-cluster Monte Carlo algorithm.

L	$\tau_{\text{int},\mathcal{E}}$	$\tau_{\text{int},\rho}$	$\tau_{\text{int},\chi}$
12	25.0(2)	22.9(1)	29.7(2)
18	57.3(5)	53.4(5)	68.4(7)
24	98.5(9)	93.0(8)	117(1)
30	147(2)	140(2)	174(2)
42	268(3)	258(3)	314(4)
60	502(6)	488(6)	580(8)
120	1531(24)	1504(23)	1728(29)
240	4962(70)	4914(69)	5285(81)
480	14430(496)	14352(492)	15779(567)

ACKNOWLEDGMENTS

This work was partially supported by the National Natural Science Foundation of China under Grant No. 10447111 and the Alexander von Humboldt Foundation of Germany (Y.D.). One of us (Y.D.) is greatly indebted to Henk W. J. Blöte, Timothy G. Garoni, and Alan D. Sokal for valuable discussions. We are grateful to NYU ITS for use of their computer cluster.

[1] R. J. Baxter, J. Phys. A **13**, L61 (1980).
[2] R. J. Baxter, *Exactly Solved Models in Statistical Mechanics* (Academic Press, San Diego, 1982).
[3] R. J. Baxter, J. Stat. Phys. **26**, 427 (1981).
[4] D. A. Huse, Phys. Rev. Lett. **49**, 1121 (1982).
[5] R. J. Baxter and P. A. Pearce, J. Phys. A **16**, 2239 (1983).
[6] W. Guo and H. W. J. Blöte, Phys. Rev. E **66**, 046140 (2002).
[7] H. C. M. Fernandes, J. J. Arenzon, and Y. Levinn, J. Chem. Phys. **126**, 114508 (2007).
[8] J. Orban and A. Bellemans, J. Chem. Phys. **49**, 363 (1968).
[9] L. K. Runnels, J. R. Craig, and H. R. Stereiffer, J. Chem. Phys. **54**, 2004 (1971).
[10] N. C. Bartelt and T. L. Einstein, Phys. Rev. B **30**, 5339 (1984).
[11] B. Nienhuis, *Phase Transitions and Critical Phenomena*, edited by C. Domb and J. L. Lebowitz (Academic Press, London, 1987), Vol. 11, p. 1, and references therein.
[12] J. L. Cardy, in *Phase Transitions and Critical Phenomena* (Ref. [11]), Vol. 11, p. 55, and references therein.
[13] A. Yamagata, Physica A **222**, 119 (1995); **231**, 495 (1996).
[14] Y. Deng and H. W. J. Blöte, Phys. Rev. E **68**, 036125 (2003).
[15] J. R. Heringa and H. W. J. Blöte, J. Phys. A **232**, 369 (1996).
[16] J. R. Heringa and H. W. J. Blöte, Phys. Rev. E **57**, 4976 (1998).
[17] C. Dress and W. Krauth, J. Phys. A **28**, L597 (1995).
[18] Y. Deng, J. R. Heringa, and H. W. J. Blöte, Phys. Rev. E **71**, 036115 (2005); Y. Deng and H. W. J. Blöte, *ibid.* **70**, 046111 (2004).
[19] R. H. Swendsen and J. S. Wang, Phys. Rev. Lett. **58**, 86 (1987).
[20] R. G. Edwards and A. D. Sokal, Phys. Rev. D **38**, 2009 (1988).
[21] J. Salas and A. D. Sokal, J. Stat. Phys. **88**, 567 (1997).
[22] X.-J. Li and A. D. Sokal, Phys. Rev. Lett. **63**, 827 (1989).
[23] J. W. Liu and E. Luijten, Phys. Rev. Lett. **93**, 247802 (2004); Phys. Rev. E **71**, 066701 (2005).